Magnetic structure and spin dynamics of the ground state of the molecular cluster $Mn_{12}O_{12}$ acetate studied by ^{55}Mn NMR

Y. Furukawa, K. Watanabe, and K. Kumagai
Division of Physics, Graduate School of Sciences, Hokkaido University, Sapporo 060-0810, Japan

F. Borsa
Department of Physics and Astronomy, Ames Laboratory, Iowa State University, Ames, Iowa 50011 and Dipartimento di Fisica "A. Volta" e Unita' INFM di Pavia, Via Bassi 6, 271000 Pavia, Italy

D. Gatteschi
Department of Chemistry, University of Florence, Via Maragliano 77, 50144 Firenze, Italy
(Received 22 Februrary 2001; published 2 August 2001)

^{55}Mn nuclear magnetic resonance (NMR) measurements have been carried out in an oriented powder sample of Mn12 acetate at low temperature (1.4–3 K) in order to investigate locally the static and dynamic magnetic properties of the molecule in its high-spin $S=10$ ground state. We report the observation of three ^{55}Mn NMR lines under zero external magnetic field. From the resonance frequency and the width of the lines we derive the internal hyperfine field and the quadrupole coupling constant at each of the three nonequivalent Mn ion sites. From the field dependence of the spectrum we obtain a direct confirmation of the standard picture, in which spin moments of Mn^{4+} ions ($S=3/2$) of the inner tetrahedron are polarized antiparallel to that of Mn^{3+} ions ($S=2$) of the outer ring with no measurable canting from the easy axis up to an applied field of 6 T. It is found that the splitting of the ^{55}Mn-NMR lines when a magnetic field is applied at low temperature allows one to monitor the off-equilibrium population of the molecules in the different low lying magnetic states. The measured nuclear spin-lattice relaxation time T_1 strongly depends on temperature and magnetic field. The behavior could be fitted well by considering the local-field fluctuations at the nuclear ^{55}Mn site due to the thermal reorientation of the total $S=10$ spin of the molecule. From the fit of the data one can derive the product of the spin-phonon coupling constant times the mean-square value of the fluctuating hyperfine field. The two constants could be estimated separately by making some assumptions. The comparison of the mean-square fluctuation from relaxation with the static hyperfine field from the spectrum suggests that nonuniform terms ($q \neq 0$) are important in describing the spin dynamics of the local Mn moments in the ground state.

DOI: 10.1103/PhysRevB.64.104401 PACS number(s): 76.60.−k, 75.45.+j, 75.50.Xx

I. INTRODUCTION

Recently much attention has been paid to molecular nanomagnets because of the observation at low temperature of slow superparamagnetic relaxation of the magnetization combined with quantum phenomena such as coherent and phonon-assisted tunneling of the magnetization and because of the consequent technological interest.[1] Among the magnetic clusters, $[Mn_{12}O_{12}(CH_3COO)_{16}(H_2O)_4]$ (henceforth abbreviated as Mn12) is one of the most investigated molecular magnet and the first where quantum tunneling phenomena have been reported.[2,3] The Mn12 cluster was first prepared and characterized using x-ray measurements by Lis.[4] Figure 1 shows the crystal structure of Mn12, where three symmetry-inequivalent Mn sites are present: Mn(1) form a tetrahedron at the center of the cluster while Mn(2) and Mn(3) occupy sites on the outside. It is widely believed that the inner four Mn(1) ions are in Mn^{4+} ionic state with $S=3/2$ while the Mn(2) and Mn(3) are in Mn^{3+} ($S=2$) state. Magnetization measurements indicate that the magnetic ground state of the cluster is a total high-spin $S=10$ state where the four inner Mn^{4+} spins ($S=3/2$) are directed antiparallel to the eight Mn^{3+} spins ($S=2$).[5] Recent polarized neutron diffraction measurements[6] have confirmed this model for the low-temperature ground state magnetic structure, although the values of the local magnetic moments along the easy axis are estimated to be -2.34 ± 0.13, 3.69 ± 0.14, and $3.79\pm0.12\mu_B$ (Bohr magnetons), for Mn(1), Mn(2), and Mn(3), respectively, which is less than predicted by the standard local spin assignment given above. This reduction has been justified by first principle calculations.[7] The total moment of the molecule is $20.56\pm0.9\ \mu_B$, which is

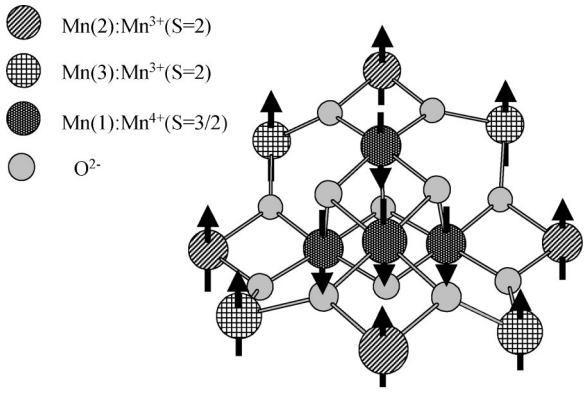

FIG. 1. Structure of Mn12 cluster and orientation of the Mn moments in the ground state according to the standard picture.

close to the value for a $S=10$ total high spin. Thus the $S=10$ description of the ground state is a good starting point even if refinements due to many-body effects may be necessary.[8]

The $S=10$ ground state is split into eleven sublevels by a strong easy-axis anisotropy, neglecting transverse hexadecupolar effects.[5] The remaining Kramers degeneracy is removed by an external magnetic field yielding energy levels for the 21 magnetic sublevels m that can be expressed as

$$E_m = -Dm^2 - Bm^4 + hm\cos\theta. \quad (1)$$

The most recent determination of the parameters obtained from neutron scattering[9,10] yielded: $D=0.55$ K and $B=1.2\times10^{-3}$ K. We will neglect here the very small nondiagonal transverse term detected in the recent experiment.[10] Assuming a gyromagnetic ratio $g=2$ one has $h=g\mu_B H/k_B=1.33H$ (K) for H in tesla and θ is the angle between the easy axis (c axis) of the cluster and the external magnetic field. Below liquid helium temperature the clusters occupy mostly the $m=\pm10$ states and the reorientation of the magnetization between these two states becomes extremely long—about a couple of months at 2 K—due to the anisotropy barrier giving rise to a pronounced superparamagnetic behavior.[11]

Nuclear magnetic resonance (NMR) is a microscopic probe suitable to investigate the internal magnetic structure of the cluster. The NMR spectrum gives us information on the hyperfine interactions of the nuclei with the local magnetic moments while the nuclear spin lattice relaxation rate (T_1^{-1}) is related to the power spectrum of the fluctuations of the local moments. Previous NMR studies of the Mn12 cluster were done by using as probes proton[12] or deuteron[13] nuclei. In view of the averaging effect over the many protons present in each cluster and the weakness of the hyperfine coupling to the Mn moments the information obtained are indirect and difficult to be interpreted. The use of the manganese nucleus as a probe of the local magnetic properties should yield much more direct information.

In this paper, we report a comprehensive study of the ^{55}Mn NMR and relaxation in Mn12 cluster at low temperature (1.4–3 K) that complements the measurements of ^{55}Mn NMR first reported by Goto and coworkers.[14] In Sec. III A, we present the results of the NMR spectrum and the field dependence of the resonance frequency for the three different lines observed from which we derive information about the hyperfine interactions and the orientation of the magnetic moments associated to the different nonequivalent Mn ions in the cluster. In Sec. III B we report the temperature and magnetic-field dependence of the nuclear relaxation rate that we compare with the predictions of a simple model describing the fluctuation spectrum of the local Mn moments in terms of the lifetime of the magnetization in the ground state due to spin-phonon coupling and possible tunneling effects.

II. EXPERIMENT

Polycrystalline samples of

$$[Mn_{12}O_{12}(CH_3COO)_{16}(H_2O)_4]\ \ 2CH_3COOH4H_2O$$

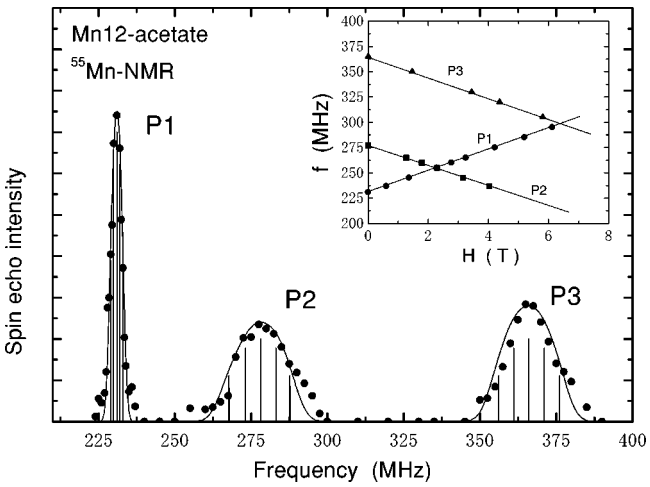

FIG. 2. ^{55}Mn-NMR spectra in Mn12 cluster measured at $H=0$ and $T=1.4$ K. Solid lines and curves in the figure are the results of simulations as described in the text. The inset shows the field dependence of the resonance frequency for each peak measured at $T=1.4$ K in thermal equilibrium state.

were prepared as described in Ref. 5. The powdered material was mixed with Stycast 1266 and allowed to set in a magnetic field of 9 T at 300 K for several hours in order to obtain a sample with rigid orientation of the crystallites with their easy axis (c axis) along the same direction (magnetic field direction). The extent of alignment of the powder can be estimated to be better than 90% from the NMR spectra discussed below and from magnetization measurements. The ^{55}Mn-NMR measurements were carried out utilizing a phase-coherent spin-echo pulse spectrometer. The spectra were obtained by plotting the spin-echo intensity at different resonance frequencies. The echo was obtained with two pulses: $\pi/2$, π in phase (Hahn echo) with a typical pulse length for the $\pi/2$ pulse of ~2 μsec. The range of temperature explored, 1.4–3 K, was obtained by adiabatic evaporation of liquid ^{4}He with the sample immersed in the liquid. The measurements done in an external magnetic field were performed in field-cooled conditions so that the system was in thermal equilibrium conditions during the measurements, except for the spectrum measurements under magnetic fields in off-equilibrium state.

III. RESULTS AND DISCUSSIONS

A. ^{55}Mn-NMR spectra

Figure 2 shows ^{55}Mn-NMR spectra under zero magnetic field at $T=1.5$ K, where the observed spectra consists of three distinct peaks, one sharp peak centered at 231 MHz (P1) and two relatively broad peaks centered at 277 MHz (P2) and 365 MHz (P3). The observation of ^{55}Mn-NMR signal in zero external magnetic field clearly indicates that the direction of Mn spin moment is frozen in the time scale of the NMR experiment (10^{-8} sec), in agreement with the superparamagnetic behavior of the magnetization (total spin) for Mn12 clusters at low temperature.[11]

The position and the width of the three peaks in the NMR spectrum in zero external magnetic field can be explained by

the combination of a large internal hyperfine field and a small quadrupole interaction. The internal field determines the resonance frequency of the lines. The quadrupole effect generates a field-independent first-order splitting of each line that, when combined with magnetic inhomogeneous broadening, yields the observed line width. The nuclear spin Hamiltonian can be expressed as[15]

$$H = H_M + H_Q = -\gamma_N h \mathbf{H}_{\rm int} \cdot \mathbf{I} + \frac{1}{6} h \nu_Q [3I_z^2 - I(I+1) + (1/2)\eta(I_+^2 + I_-^2)], \quad (2)$$

where $\nu_Q = (3/2)e^2 qQ/I(2I-1)$. The electric field gradient (EFG) tensor is defined in its principal axis system, *X*, *Y*, *Z*, with the maximum component V_{ZZ} and the asymmetry parameter $\eta = (V_{XX} - V_{YY})/V_{ZZ}$. The local EFG symmetry at the ^{55}Mn site is due to the oxygen coordination around the Mn ion. For the Mn^{4+} site one has a slightly trigonally distorted octahedral coordination while for the Mn^{3+} site the oxygen are in an elongated octahedral coordination due to Jahn-Teller distortion.[5] In both cases the asymmetry parameter is close to zero [$\eta = 0$ in Eq. (2)]. In first order perturbation theory (valid for $H_M \gg H_Q$) one has for the Zeeman nuclear energy levels ($I = 5/2$),[15]

$$E_m/h = -\frac{\gamma_N}{2\pi} H_{int} m - \frac{1}{12} \nu_Q (3\cos^2\theta - 1)\left[3m^2 - \frac{35}{4}\right]. \quad (3)$$

Thus the ^{55}Mn spectrum is composed of a central line at $\nu_R = (\gamma_N/2\pi)H_{\rm int}$ and two pairs of satellite lines at $\nu_R^1 = (\gamma_N/2\pi)H_{\rm int} \pm (\nu_Q/2)(3\cos^2\theta - 1)$ and $\nu_R^2 = (\gamma_N/2\pi)H_{\rm int} \pm \nu_Q(3\cos^2\theta - 1)$, respectively, where θ is the angle between the internal magnetic field and the local symmetry axis of the EFG tensor. In order to confirm the presence of first-order quadrupole splitting of the line we measured the spin-echo decay time T_2 at different points of the line P2 (see Fig. 2). The value found at the center of the line ($T_2 = 630$ μsec at $T = 1.4$ K) is shorter than at the tail ($T_2 = 750$ μsec) as expected for irradiation of the central line and of the satellite line, respectively, of a quadrupole split spectrum.

From the frequency of the center of each of the three peaks in Fig. 2 one derives: $H_{\rm int} \sim |220|$ kOe for P1, $H_{\rm int} \sim |264|$ kOe for P2, and $H_{\rm int} \sim |347|$ kOe for P3. From the width of each peak we get for the line P1 (Mn^{4+}) $\nu_Q(3\cos^2\theta_1 - 1) \sim 2$ MHz, while for the lines P2 and P3 we get $\nu_Q(3\cos^2\theta_{2,3} - 1) \sim 10$ MHz. The vertical lines for each peak in the figure indicate the peak positions of quadrupole split lines for Mn-NMR signal using the above parameters in Eq. (3) and the solid curves are the results of fits with an approximate broadening of 5 MHz or less for each line. The broadening of each line appears to be of inhomogeneous kind from the formation of Hahn echoes and is much bigger than expected from nuclear-nuclear dipolar interaction. It should probably be ascribed to a combination of the intramolecular dipolar fields generated by the Mn moments other than the one containing the given nucleus and intermolecular dipolar fields due to the total spin magnetization of the surrounding molecules. The assignment of the angles θ for the different Mn sites is not totally unambiguous. For the four Mn^{4+}, one can assume $\theta = 0$ ($Z \| H_{\rm int}$) that leads to $\nu_Q \sim 1$ MHz. For the eight Mn^{3+} ions one can assume as the direction of the local symmetry axis the axis of elongation of the oxygen octahedron surrounding the Mn ion. In this case the angle between the EFG local principal axis Z and the internal field (same as the easy axis) can be estimated to be $\theta_2 = 11°$ for Mn(2) and $\theta_3 = 36°$ for Mn(3) (see Fig. 1). This leads to $\nu_Q \sim 5.3$ MHz and 10.4 MHz respectively for the two different Mn^{3+} sites without knowing which one is which.

The narrow line P1 with the small quadrupole coupling constant is consistent with the symmetric octahedral coordination of Mn^{4+}. The difference by a factor of two of the quadrupole coupling constant for the two different Mn^{3+} sites Mn(2) and Mn(3) (lines P2 and P3) is consistent with the different distortion of the octahedron namely $c/a \sim 1.11$ and $c/a \sim 1.16$, respectively.[4] It must also be recalled that in the coordination polyhedron of one group of manganese(III) there are two oxides and four oxygens of acetate ligands, while in the other group of manganese(III) one of the acetates is replaced by a water molecule. The above assignment is confirmed by the magnetic field dependence of the spectrum as will be described later. The observed spectrum is in good agreement with the one reported by Goto *et al.*,[14] in which a same signal assignment has been done.

The resonance frequency of the three signals in the spectrum (Fig. 2) was followed as a function of the external magnetic field applied along the c easy axis. The results are shown in the inset of Fig. 2. With increasing external magnetic field $H_{\rm ext}$, the peak coming from Mn^{4+} ions shifts to higher frequency while the other two peaks of Mn^{3+} ions move to lower frequency. Since the resonance frequency is proportional to the vector sum of internal field and external field, $\omega_R = \gamma_N(\mathbf{H}_{\rm int} + \mathbf{H}_{\rm ext})$, this result indicates that the direction of the internal field at the nucleus in Mn^{3+} is opposite to that in Mn^{4+} ions.

The internal fields at the Mn nucleus are proportional to the on-site electron-spin momentum, i.e., $H_{\rm int} = A_{\rm hf}\langle S \rangle$, where $A_{\rm hf}$ is a hyperfine coupling constant and $\langle S \rangle$ is the Mn local-ordered spin. The hyperfine constant at the Mn nuclear site can in principle result from the sum of different contributions both on site (core polarization, contact term, nuclear-electron dipolar interaction, orbital contribution) and coming from neighboring magnetic ions (dipolar interaction, transferred hyperfine interactions).[16,17] In practice, since the magnetic *d* electrons are localized on the Mn ions the dominant contribution is the core polarization term.[18] The dipolar contribution, which is proportional to $\langle r^{-3} \rangle$ and depends on the relative orientation of the nuclear polarization and the electronic one, can have some importance for Mn(III). Since the two different groups of manganese(III) ions have different angles between elongation axis and easy axis it is possible that at least part of the difference in resonance frequency may be a consequence of this factor. Measurements of hyperfine fields using electron-nuclear double resonance technique have yielded values ranging from $A_{\rm hf} = -8.15$ T/μ_B for Mn^{2+} ions in CaO (Ref. 19) to $A_{\rm hf} = -9.9$ T/μ_B for Mn^{4+} in Al_2O_3 (Ref. 20) where the minus sign is character-

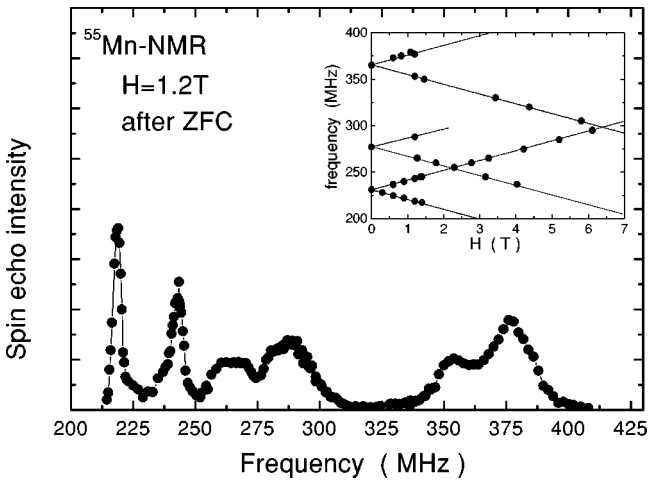

FIG. 3. ^{55}Mn-NMR spectra at $H=1.2$ T after zero-field cooling to 1.4 K (off-equilibrium state). The inset shows the field dependence of the resonance frequency for each split peak.

istic of core polarization fields. If we assume that the internal field at the ^{55}Mn sites in Mn12 is due to core polarization only we derive from the positions of the NMR peaks in Fig. 2: $A_{\rm hf}=-8.46$ T/$\mu_{\rm B}$ for P1 (Mn^{4+} ions) $A_{\rm hf}=-7.32$ T/$\mu_{\rm B}$ for P2, and $A_{\rm hf}=-9.65$ T/$\mu_{\rm B}$ for P3 (Mn^{3+} ions) respectively, with the assumption of a spin moment of $2.6\mu_{\rm B}$ for Mn^{4+} and $3.6\mu_{\rm B}$ for Mn^{3+}. Since these values are close to the core polarization fields in Mn ions reported above we can conclude that the dominant hyperfine field at the ^{55}Mn nuclear site in Mn12 is indeed due to core polarization. Thus, $H_{\rm int}$ is negative and the direction of the internal fields at nuclear sites is opposite to that of the Mn spin moment. From the behavior of the resonance frequency as a function of external field in Fig. 2 (inset), one concludes that the spin direction of the Mn^{4+} ions is antiparallel to the external magnetic field (i.e., easy axis), while that of Mn^{3+} ions is parallel to the external field. This is a direct confirmation of the spin structure for inner magnetic structure of the cluster shown in Fig. 1.

The slope of the field dependences of the resonance frequency is $\sim|10.5|$ MHz/T for each peak, which is exactly the same as the gyromagnetic ratio $\gamma_{\rm N}/2\pi$ of ^{55}Mn nucleus. This result suggests that each Mn spin moment aligns along the $H_{\rm ext}$ direction without any appreciable deviation and that the spin moments on Mn^{4+} ions do not develop any measurable canting components up to 6 T.

When the oriented sample is cooled down to 1.4 K in an external magnetic field applied along the easy axis, most of the clusters occupy the $m=-10$ sublevel. For this field-cooled condition the NMR spectrum is the one shown in Fig. 2. If we apply the magnetic field to the oriented sample after cooling to 1.4 K whose condition is corresponding to an off-equilibrium state, the observed spectrum is quite different. In zero-field cooling each peak splits into two peaks with increasing magnetic field as shown in Fig. 3. One of the split peaks moves the same way as shown in the inset of Fig. 2, while the other shifts in the opposite direction but with the same field-dependent slope as shown in an inset of Fig. 3 including the data shown in the inset of Fig. 2. This can be explained by considering the two clusters occupying the $m=\pm 10$ states with opposite magnetization. At this low temperature the relaxation time of the magnetization is extremely long so that clusters occupying the $m=10$ excited state cannot relax to $m=-10$ that has lower energy in the external magnetic field. Thus the two split peaks correspond to ^{55}Mn belonging to the two clusters in different magnetic sublevels. The observation of the split peaks is a direct confirmation of the Kramers degeneracy of $S=10$ sublevels due to the crystal anisotropy. This circumstance allows one to investigate the local magnetic properties of the different sublevels and the long relaxation time of the magnetization of the molecule in a way similar to what was done by using proton NMR.[21]

Interestingly, NMR signal intensity for excited $m=10$ sublevels is larger than that of $m=-10$ sublevels. Since the signal intensity is proportional to the number of Mn nuclei occupying the sublevels, this result suggests that energy level of $m=10$ sublevel is a little bit lower than that of $m=-10$ sublevel. Assuming the signal intensity ratio of $I_{m=10}/I_{m=-10}\sim 1.3$, the difference in energy of the levels is estimated to be ~ 0.4 K, which corresponds to an external magnetic field of ~ 150 Oe antiparallel to the easy axis. This small magnetic field could be due to dipolar field from the neighboring clusters. This small hyperfine field is very relevant for the problem of quantum tunneling of the magnetization because it lifts the degeneracy of the $m=+10$ and $m=-10$ levels in zero external field.

B. ^{55}Mn spin-lattice relaxation time

Nuclear spin lattice relaxation time (T_1) was measured for each Mn site by monitoring the recovery of the nuclear-magnetization after a saturating sequence of rf pulses. In the case of ^{55}Mn ($I=5/2$), the nuclear magnetization recovery law for saturation of the central line only is given by[22]

$$\frac{[M(\infty)-M(t)]}{M(\infty)}=\frac{1}{35}\exp\left(-\frac{t}{T_1}\right)+\frac{8}{45}\exp\left(-\frac{6t}{T_1}\right)+\frac{50}{63}\exp\left(-\frac{15t}{T_1}\right), \quad (4)$$

where $M(t)$ is the magnetization at a time t after the saturation sequence. On the other hand, in the limit of saturation of both central line and satellite lines the recovery should be exponential, i.e., $\exp(-t/T_1)$.[22] The experimental conditions in our case are somewhat intermediate because the line is too broad to obtain complete saturation but at the same time the central line and satellite lines overlap so that one cannot achieve selective saturation of the central line (see Fig. 2). Thus the recovery law departs from Eq. (4) particularly at long times. However, by limiting the fit to the initial part of the recovery that is dominated by the third term in Eq. (4) one can extract the relaxation time T_1. The results as a function of temperature are shown in Fig. 4 and the ones as a function of field at 1.4 K are shown in Fig. 5.

Before analyzing the data we note that the temperature dependence of T_1 is the same for the three NMR lines P1, P2, P3 within experimental error. This is apparent from the

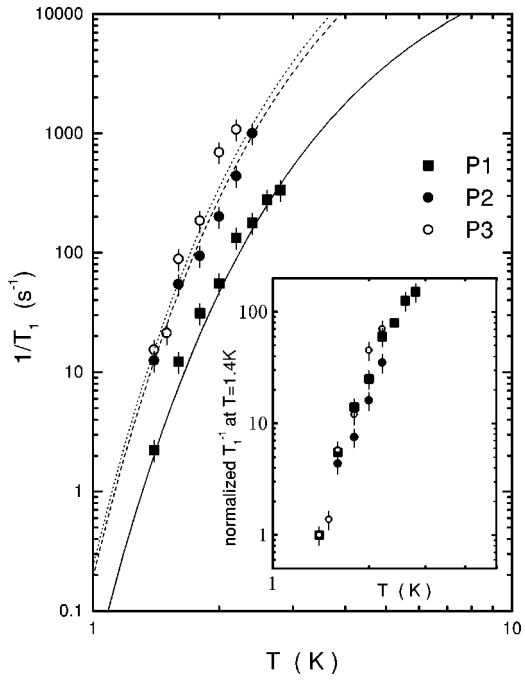

FIG. 4. Temperature dependence of T_1^{-1} for each Mn site. Solid curves are fitting curves according to Eq. (8) with the choice of parameters discussed in the text. The inset shows the temperature dependence of T_1^{-1} for the three peaks renormalized at the same value at $T=1.4$ K.

inset in Fig. 4 where the data for the three peaks have been normalized to the same value at 1.4 K. We are led to conclude that the spin dynamics of the local Mn moments is completely correlated as expected if it is driven by the fluctuations of the total spin moment $S=10$ of the ground state of the molecular cluster.

In order to fit the data we will adopt a simple phenomenological model that proved to be successful in explaining the μSR results in Mn12.[23] In this model it is assumed that the fluctuations of the total spin $S=10$ due to changes from

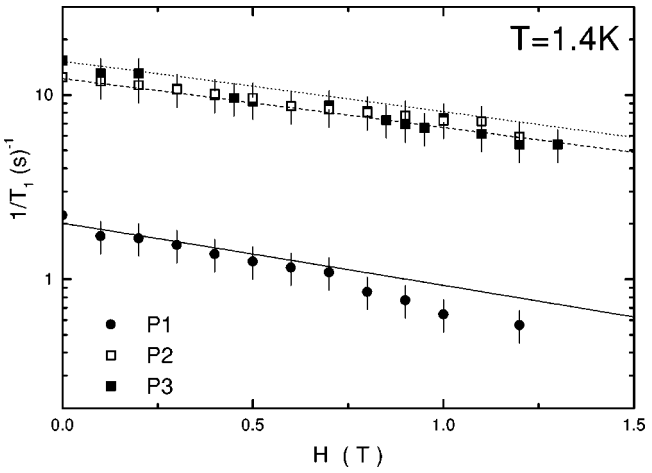

FIG. 5. Field dependence of T_1^{-1} for each Mn site measured at $T=1.4$ K. The solid lines are theoretical curves predicted by using the same parameters as in the temperature dependence fits in Fig. 4 (see text).

the magnetic ground state $m=-10$ to excited states gives rise to changes in the transverse local field, $h_{\pm}(t)$, at the nuclear sites via the hyperfine interaction between the nuclei and the local electronic spins. Accordingly, the resultant expression for nuclear spin-lattice relaxation time is given by[15,23]

$$\frac{1}{T_1}=\frac{1}{2}\gamma_N^2\int\langle h_{\pm}(t)h_{\pm}(0)\rangle\exp(i\omega_N t)dt$$

$$=\frac{A}{Z}\sum_{m=+10}^{-10}\frac{\tau_m\exp\left(-\frac{E_m}{k_BT}\right)}{1+\omega_N^2\tau_m^2}, \quad (5)$$

where Z is a partition function, τ_m is the average lifetime of the mth sublevels of $S=10$, and ω_N is resonance frequency. The lifetime τ_m for each individual mth state is determined by the probability of a transition from m to $m\pm1$ and to $m\pm2$.

$$\frac{1}{\tau_m}=W_{m\to m+1}+W_{m\to m-1}+W_{m\to m+2}+W_{m\to m-2}. \quad (6)$$

By assuming that the transition probabilities are due to spin-phonon interaction one can express them in terms of the energy level differences as[24,25]

$$W_{m\to m\pm1}=W_{\pm1}=Cs_{\pm1}\frac{(E_{m\pm1}-E_m)^3}{\exp[(E_{m\pm1}-E_m)/k_BT]-1},$$

$$W_{m\to m\pm2}=W_{\pm2}=1.06Cs_{\pm2}\frac{(E_{m\pm2}-E_m)^3}{\exp[(E_{m\pm2}-E_m)k_BT]-1}, \quad (7)$$

where

$$s_{\pm1}=(s\mp m)(s\pm m+1)(2m+1)^2,$$

$$s_{\pm2}=(s\mp m)(s\pm m+1)(s\mp m-1)(s\pm m+2). \quad (7')$$

The parameter C in Eq. (7) is given by $D'^2/(12\pi\rho v^5\hbar^4)$ with ρ the mass density and v the sound velocity. The spin-phonon coupling constant D' was shown to coincide with the axial magnetic anisotropy D [see Eq. (1)] for the case of Mn12.[24]

In the narrow temperature range (1.4–3 K) where the NMR signal can be detected, only the ground state ($m=\pm10$) has significant occupation. Thus the expression for the relaxation rate obtained from Eqs. (5), (6), and (7) and by using the energy levels in Eq. (1) can be greatly simplified. The formula valid within a few percent up to $3\sim4$ K is

$$\frac{1}{T_1}=AC2.2\times10^7\exp(-14.58/T)\omega_N^{-2} \quad \text{(rad/sec)}. \quad (8)$$

As seen from Eq. (8) the two fitting parameters cannot be determined independently on this narrow temperature range. The theoretical curves in Fig. 3 were obtained from Eq. (8) by choosing the following values: $AC=6.4$

$\times 10^{15}$ [(rad Hz)^3/K^3] for $P1$, 5.6×10^{16} for $P2$, and 1.2×10^{17} for $P3$. The value of $C=D'^2/(12\pi\rho v^5\hbar^4)$ can be estimated by taking $D'=D=0.55$ K, $\rho=1.83$ g/cm^3,[4] and $v=2\times 10^5$ cm/sec that yields $C\simeq 0.6$ Hz/K^3. The above value for the sound velocity was estimated from the value of Debye temperature $\Theta_D=38$ K (Ref. 26) using a relation of $k_B\Theta_D=\hbar v k_D$ with $k_D^3=6\pi^2/V_0$ where V_0 is the unit cell volume of 3716 Å^3. Then the hyperfine coupling constant at the ^{55}Mn nuclei are

$$A=1.1\times 10^{16}\ (\text{rad Hz})^2 \ \text{for}\ P1\ (\text{Mn}^{4+}),$$

$$A=9.3\times 10^{16}\ (\text{rad Hz})^2 \ \text{for}\ P2\ (\text{Mn}^{3+}),$$

$$A=2.0\times 10^{17}\ (\text{rad Hz})^2 \ \text{for}\ P3\ (\text{Mn}^{3+}). \qquad (9)$$

In the simple case where uniform fluctuations with $q\sim 0$ (q: wave vector) dominate the nuclear relaxation, one would expect that the coupling constants A for each peak should be proportional to square of the internal static field as derived from the spectrum in Fig. 2, i.e., $P1:P2:P3=1:1.4:2.5$. The ratios obtained from the values in Eq. (9) are instead $P1:P2:P3=1:8.5:18.1$. This discrepancy suggests that nonuniform $q\neq 0$ components may be important in describing the fluctuations of the local-Mn moments that determine the fluctuation of the total magnetization in its ground state.

In order to investigate the possible role of quantum tunneling on the fluctuations of the magnetization we measured the field dependence of T_1 in thermal equilibrium state. Figure 5 shows H dependence of T_1 for each Mn site measured at $T=1.4$ K. With the increasing of the external magnetic field H_{ext} that is applied along the easy axis of the cluster, T_1^{-1} for all Mn sites decreases. The solid lines in Fig. 5 are the curves obtained from Eqs. (5), (6), and (7), and the energy levels in Eq. (1) with the same values of the parameters used to fit the temperature dependence in Fig. 4. The field dependence appears to be well described by the thermal-fluctuation model and without any anomaly due to the effect of quantum tunneling of the magnetization around the level crossing fields 0.45, 0.9, and 1.35 T. Further measurements at different temperatures and in off-equilibrium state are needed to investigate quantum tunneling. It is noted that the overall decrease of T_1^{-1} on increasing magnetic field is not trivial due to the change of $\omega_N=\gamma_N H$ in Eq. (5) (the effect is negligible), but rather to the field dependence of the energy spacing [Eq. (1)] that affects the spin-phonon transition probability [Eq. (7)].

IV. SUMMARY AND CONCLUSIONS

We have carried out ^{55}Mn NMR at low temperature in order to investigate the internal structure of the magnetic ground state of Mn12 cluster. From the analysis of the NMR spectrum and its field dependence we could confirm the standard picture for the internal magnetic structure of the core, in which the local-spin moments of Mn^{4+} ions ($S=3/2$) of the inner tetrahedron are polarized antiparallel to that of Mn^{3+} ions ($S=2$) for the outer ring with both set of moments aligned along the easy axis without appreciable canting up to 6 T. The internal field at the ^{55}Mn nuclear site is determined and shown to be dominated by a negative core polarization hyperfine interaction due to the $3d$ electrons localized on the Mn ions. The quadrupole coupling constant at the different Mn sites is determined and it is found to be a parameter very sensitive to the degree of distortion of the octahedral configuration of the oxygens coordinated around the Mn central ion. The nuclear spin-lattice relaxation time T_1 is found to depend strongly on temperature (1.4–3 K) and magnetic field (0–1.5 T). The behavior can be fitted well by using a simple model based on the assumption that the local field fluctuation at the nuclear site is due to the fluctuation of the orientation of the total $s=10$ spin of the molecule. The fluctuation appears to be explained almost entirely in terms of spin-phonon coupling. It is found that when the sample is prepared in off-equilibrium conditions, with half of the clusters with the magnetization parallel to the external field and half antiparallel to it, each NMR line split into two components that can be investigated separately. This effect appears to be most promising for further studies, particularly in connection with the problem of quantum tunneling of the magnetization.

ACKNOWLEDGMENTS

We are grateful to T. Goto, A. Lascialfari, Z. H. Jang, V. Dobrovitski, P. Kogerler, and A. Kawamoto for useful discussions and suggestions. Ames Laboratory is operated for U.S. Department of Energy by Iowa State University under Contract No. W-7405-Eng-82. This work at Ames Laboratory was supported by the Director for Energy Research, Office of Basic Energy Sciences. The present work was supported in part by a Grant-in-Aid for Scientific Research on Priority Areas from the Ministry of Education, Science, Sports, and Culture of Japan.

[1] See contributions in *Quantum Tunneling of Magnetization*, edited by L. Gunther and B. Barbara (Kluwer, Dordrecht, 1995).
[2] J. R. Friedman, M. P. Sarachik, J. Tejada, and R. Ziolo, Phys. Rev. Lett. **76**, 3830 (1996).
[3] L. Thomas, F. Lionti, R. Ballou, D. Gatteschi, R. Sessoli, and B. Barbara, Nature (London) **383**, 145 (1996).
[4] T. Lis, Acta Crystallogr., Sect. B: Struct. Crystallogr. Cryst. Chem. **36**, 2042 (1980).
[5] R. R. Sessoli, H. L. Tsai, A. R. Schake, S. Wang, J. B. Vincent, K. Folting, D. Gatteschi, G. Christou, and D. N. Hendrickson, J. Am. Chem. Soc. **115**, 1804 (1993).
[6] R. A. Robinson, P. J. Brown, D. N. Argyriou, D. N. Hendrickson, and S. M. J. Aubin, J. Phys.: Condens. Matter **12**, 2805 (2000).
[7] M. R. Pederson and S. N. Khanna, Phys. Rev. B **60**, 9566 (1999).

[8] M. I. Katsnelson, V. V. Dobrovitski, and B. N. Harmon, Phys. Rev. B **59**, 6919 (1999).
[9] Y. Zhong, M. P. Sarachik, J. R. Friedman, R. A. Robinson, T. M. Kelly, H. Nakotte, C. Christianson, F. Trouw, S. M. J. Aubin, and D. N. Hendrickson, J. Appl. Phys. **85**, 5636 (1999).
[10] I. Mirebeau, M. Hennion, H. Casalta, H. Andres, H. U. Gudel, A. V. Irodova, and A. Caneschi, Phys. Rev. Lett. **83**, 628 (1999).
[11] R. Sessoli, D. Gatteschi, A. Caneschi, and M. A. Novak, Nature (London) **365**, 141 (1993).
[12] Y. Furukawa, K. Watanabe, K. Kumagai, Z. H. Jang, and A. Lascialfari, F. Borsa, and D. Gatteschi, Phys. Rev. B **62**, 14 246 (2000); see also, A. Lascialfari, D. Gatteschi, F. Borsa, A. Shastri, Z. H. Jang, and P. Carretta, *ibid.* **57**, 514 (1998).
[13] D. Arcon, J. Dolinsek, T. Apih, and R. Blinc, Phys. Rev. B **58**, R2941 (1998).
[14] T. Goto, T. Kubo, T. Koshiba, J. Arai, Y. Fujii, A. Oyamada, K. Takeda, and K. Awaga, Physica B (Amsterdam) **284B-288B**, 1227 (2000).
[15] A. Abragam, *Principles of Nuclear Magnetism* (Clarendon Press, Oxford, 1961).
[16] G. C. Carter, L. H. Bennett, and D. J. Kahan, *Metallic Shifts in NMR*, Progress in Material Science Vol. 20 (Pergamon Press, New York, 1977); see also J. J. Van der Klink and H. B. Brom, Progress in Nuclear Magnetic Resonance Spectroscopy, **86**, 89 (2000).
[17] M. Zheng and G. C. Dismukes, Inorg. Chem. **35**, 3307 (1996).
[18] R. E. Watson and A. J. Freeman, in *Hyperfine Interactions*, edited by A. J. Freeman and R. B. Frankel (Academic Press, New York, 1967), p. 53.
[19] W. B. Mims, G. E. Devlin, S. Geschwind, and V. Jaccarino, Phys. Lett. A **24**, 481 (1967).
[20] S. Geschwind, in *Hyperfine Interactions*, edited by A. J. Freeman and R. B. Frankel (Academic Press, New York, 1967).
[21] Z. H. Jang, A. Lascialfari, F. Borsa, and D. Gatteschi, Phys. Rev. Lett. **84**, 2977 (2000); see also Furukawa *et al.* (Ref. 12).
[22] E. R. Andrew and D. P. Tunstall, Proc. Phys. Soc. London **78**, 1 (1961).
[23] A. Lascialfari, Z. H. Jang, F. Borsa, P. Carretta, and D. Gatteschi, Phys. Rev. Lett. **81**, 3773 (1998).
[24] M. N. Leuenberger and D. Loss, Phys. Rev. B **61**, 1286 (2000).
[25] J. Villain, F. Hartmann-Boutron, R. Sessoli, and A. Rettori, Europhys. Lett. **27**, 537 (1994); see also, F. Hartmann-Boutron, P. Politi, and J. Villain, Int. J. Mod. Phys. **10**, 2577 (1996).
[26] A. M. Gomes, M. A. Novak, R. Sessoli, A. Caneschi, and D. Gatteschi, Phys. Rev. B **57**, 5021 (1998).